sustainability

MDPI

Article

Evolution and Prediction of Landscape Pattern and Habitat Quality Based on CA-Markov and InVEST Model in Hubei Section of Three Gorges Reservoir Area (TGRA)

Lin Chu [1,2], Tiancheng Sun [1,2], Tianwei Wang [1,2,*], Zhaoxia Li [1,2] and Chongfa Cai [1,2]

1 Key Laboratory of Arable Land Conservation (Middle and Lower Reaches of Yangtze River) of the Ministry of Agriculture, Soil and Water Conservation Research Centre, Huazhong Agricultural University, Wuhan 430070, China; chulin@mail.hzau.edu.cn (L.C.); tiancheng_hzau@sina.com (T.S.); zxli@mail.hzau.edu.cn (Z.L.); cfcai@mail.hzau.edu.cn (C.C.)

2 College of Resources and Environment, Huazhong Agricultural University, Wuhan 430070, China

* Correspondence: wangtianwei@webmail.hzau.edu.cn

Received: 25 August 2018; Accepted: 19 October 2018; Published: 24 October 2018

Abstract: The spatial pattern of landscape has great influence on the biodiversity provided by ecosystem. Understanding the impact of landscape pattern dynamics on habitat quality is significant in regional biodiversity conservation, ensuring ecological security guarantee, and maintaining the ecological environmental sustainability. Here, combining CA-Markov and InVEST model, we investigated the evolution of landscape pattern and habitat quality, and presented an explanation for variability of biodiversity linked to landscape pattern in Hubei section of Three Gorges Reservoir Area (TGRA). The spatial-temporal evolution characteristic of landscape pattern from 1990 to 2010 were analyzed by Markov chain. Then, the spatial pattern of habitat quality and its variation in three phases were computed by InVEST model. The driving force for landscape variation was explored by using Logistic regression analysis. Next, the CA-Markov model was used to simulate the future landscape pattern in 2020. Finally, future habitat quality maps were obtained by InVEST model predicted landscape maps. The results concluded that, the overall landscape pattern has changed slightly from 1990 to 2010. Woodland, waters and construction land had the greatest variations in proportion among the landscape types. The area of woodland has been decreasing gradually below the average elevation of 140 m, and the area of waters and construction land increased sharply. Logistics regression results indicated that terrain and climate were the most influencing natural factors compared with human factors. The Kappa coefficient reached 0.92, indicating that CA-Markov model had a good performance in future landscape prediction by adding nighttime light data as restriction factor. The biodiversity has been declining over the past 20 years due to the habitat degradation and landscape pattern variation. Overall, the maximum values of habitat degradation index were 0.1188, 0.1194 and 0.1195 respectively, showing a continuously increasing trend from 1990 to 2010. Main urban areas of Yichang city and its surrounding areas has higher habitat degradation index. The average values of habitat quality index of the whole region were 0.8563, 0.8529 and 0.8515 respectively, showing a continuously decreasing trend. The lower habitat quality index mainly located in the urban land as well as the main and tributary banks of the Yangtze River. Under the business as usual scenario, habitat quality continued to maintain the variation trend of the previous decade, showing a reducing habitat quality index and an increasing area of artificial surface. Under the ecological protection scenario, the variation of habitat quality in this scenario represented reverse trend to the previous decade, exhibiting an increase of habitat quality index and an increasing area of woodland and grassland. Construction of Three Gorges Dam, impoundment of Three Gorges Reservoir (TGR), resettlement of Three Gorges Project and urbanization were the most explanatory driving forces for landscape variation and degradation of habitat quality. The research may be useful for understanding the impact of landscape pattern dynamics on biodiversity, and provide scientific basis for optimizing regional natural environment, as well as effective decision-making support to local government for landscape planning and biodiversity conservation.

Keywords: landscape pattern; InVEST model; habitat quality; CA-Markov model; logistic regression analysis; Three Gorges Reservoir Area (TGRA)

1. Introduction

As an important part and one of the major causes of global change, landscape pattern has great influences on ecosystems and the goods and services they provide to people ("ecosystem services") [1], the change of which will lead to variations in lots of natural phenomena and ecological processes [2,3]. The term "ecosystem services" was used quite broadly to include any ecosystem process or function that contributes to human [4]. Biodiversity is intimately linked to the production of ecosystem services. As a proxy for biodiversity, habitat quality refers to the ability of the environment to provide conditions appropriate for individual and population persistence, ranging from low to medium to high, resources available for survival, reproduction, and population persistence, respectively [5]. Generally, the spatial landscape pattern can reflect the regional quality of ecological environment, and they affect each other, interact with each other, and are closely related [6]. Changes in landscape will cause corresponding changes in the ecosystem services [7–9]. By studying the spatial and temporal changes of landscape pattern, we can obtain the corresponding changes in biodiversity. For example, landscape transition from woodland to construction land has a great impact on regional biodiversity, which would cut off the spatial connectivity [10,11]. The Three Gorges Reservoir Area (TGRA) is considered to be one of the most important biodiversity hotspots in China [12]. The construction of the Three Gorges Dam has huge effects on both the environment and society. Evidence from many sources builds an overwhelming picture of pervasive biodiversity decline in this region after the completion of the Three Gorges Project [13–15]. This serious consequence for biodiversity has prompted a wide-ranging response from both governments and civil society. Therefore, analyzing the spatial and temporal changes of landscape pattern in past, and exploring the impact of landscape pattern dynamics on biodiversity are beneficial to formulate land use management strategy scientifically and effectively, which can guide the sustainable development of regional society and economy, maintain regional biodiversity, and ensure regional ecological security [16].

Changes in landscape pattern can be analyzed and simulated by various models, such as GIS-optimization modeling [17], random prediction model [18], empirical regression model [19], Cellular Automata (CA) [20,21], and so on. CA is one of the most representative geo-models, which is widely used in many fields such as land use, geomorphologic evolution, and urban expansion [22]. The CA-Markov model synthesizes the ability of CA model in simulating spatial changes in complex systems and the advantage of Markov model in long-term forecasting, which improves the prediction precision of the land use types transformation, and effectively simulates the spatial variation of land use structure [23]. The CA-Markov model, as a scientific and practical geo-model, is broadly applied to modelling and realistic prediction of land-use patterns. Based on cellular automata, Batty et al. [24] proposed a Dynamic Urban Evolution Model (DUEM), and systematically and effectively simulated urban expansion. Nourqolipour et al. [25] simulated spatial patterns of oil palm expansion by spatial and temporal prediction model integrating CA model, multi-criteria evaluation (MCE), and Markov chain (MC) in the Kuala Langat district, Malaysia. The results from above researches and other applications all demonstrated the effectiveness of CA-Markov model, which has a common applicability for modelling and realistic prediction of landscape patterns.

Changes in landscape pattern will lead to corresponding changes in the composition of ecosystem, and biodiversity. The change of habitat quality can directly exhibit the regional change of biodiversity and landscape pattern. The changes ecological processes are of great significance to regional maintenance of ecosystem service function and sustainable management. There were many models developed to evaluate the function of ecosystems services, such as Multiscale Integrated Models of Ecosystem Services (MIMES) [26], Artificial Intelligence for Ecosystem Services [27], Biodiversity module in Integrated Valuation of Ecosystem Services and Tradeoffs model (InVEST) [28] and so on. InVEST was developed as part of the Natural Capital Project [29], a partnership between Stanford University, the University of Minnesota, The Nature Conservancy, and World Wildlife Fund in 2007, whose aim is to provides a powerful tool for simultaneously quantifying and valuing multiple ecosystem services generated by a landscape. InVEST can evaluate various service functions of ecosystems such as biodiversity, soil conservation and carbon reserves, with advantages of less input data, accurate output data and intuitive spatial visualization. InVEST thus was widely used by its low application cost, high evaluation accuracy, and strong spatial analysis functions, which has been successfully applied to comprehensive assessment of the ecosystems in different areas [30–32]. Patterns in biodiversity are inherently spatial, therefore, which can be estimated by analyzing landscape maps in conjunction with threats. The above researches all obtained good evaluation results, and the InVEST model is proved scientific and effective.

CA-Markov model and InVEST have achieved effective results in their respective fields, less research has been done about the combination of two above models. By varying landscape and evaluating the output from InVEST, we can provide useful information to managers and policy-makers weighing the tradeoffs in ecosystem services, biodiversity conservation, and other landscape objectives. The Three Gorges Project is the largest hydropower project in the world today, the construction of which brings enormous benefits of flood control, electricity generation, shipping and water supply. Likewise, it has a long-term but far-reaching impact on the ecology and environment of the reservoir area and the whole basin. The ecological and environmental impact of the Three-Gorges Project has been the focus of all worlds' attention. As the special ecological functional zone, ecological security status of TGRA concerns social and economic sustainable development of the whole Yangtze River basin even the whole China. Owing to abundant in energy, resources and biodiversity, Hubei Section of TGRA has become the essential area of natural environment construction. Many scholars have studied the status of natural environment and the ecosystem health in this region, including ecological environment sensitivity, ecosystem health condition, soil erosion sensitivity and so on [33,34].

To better understand the impact of spatial and temporal dynamics in landscape pattern on biodiversity in Hubei Section of TGRA, it is important to extract the landscape pattern and calculate the habitat quality. This study therefore aimed to investigate and predict landscape pattern and habitat quality by combining CA-Markov model and InVEST model, and explore biodiversity responses under the influence of landscape pattern dynamics. Within the context of biodiversity decline, this study is of practical implications for regional biodiversity conservation, natural environment protection and economic sustainable development.

2. Materials and Methods

2.1. Study Area

Hubei section of Three Gorges Reservoir Area (TGRA) is located in the middle reaches of the Yangtze River, which lies at the head of the TGRA. The Hubei section of TGRA covers five parts (Yiling districts, main urban areas of Yichang city, Zigui county, Xingshan county and Badong county), extending from 110.06° to 111.65° E longitude and 31.06° to 31.56° N latitude (Figure 1). The total area of this land is approximately 11,895 km^2, with a population of 1.48 million people. Mountains and hills are the dominant terrain, with a summit that reaches 1000 to 2000 m. In addition to Yangtze River, some headwater rivers and streams are located in northern parts of Badong county, southern parts of Xingshan county and southeastern part of Yiling districts. This region has a typical subtropical monsoon climate with an annual average precipitation from 1000 to 1400 mm. Sub-tropical evergreen broad-leaved forest and warm coniferous forest are the main vegetation types. The soil type mainly includes yellow brown soil, rock soil, yellow soil, and purple soil.

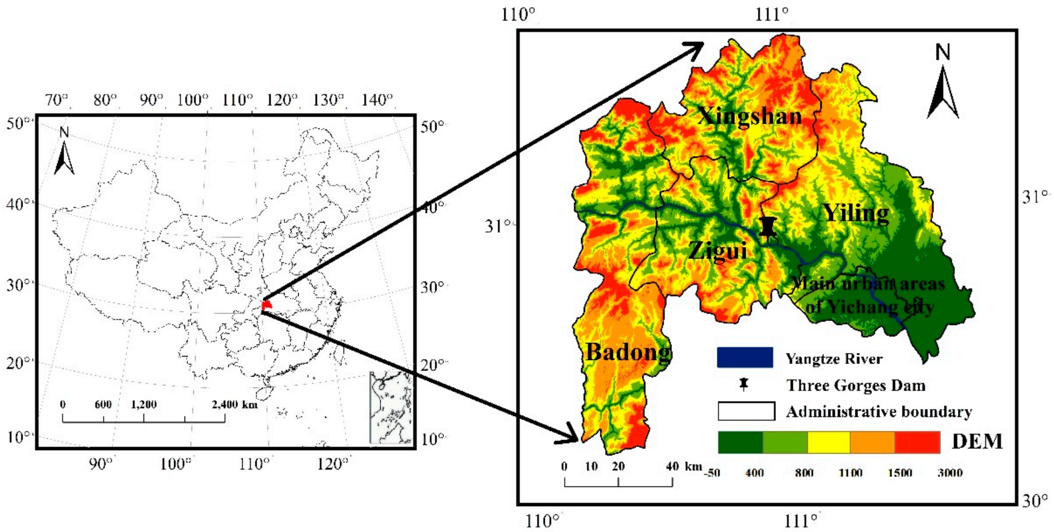

Figure 1. Geographic location of study area.

The study region is situated in the transition zone from the second to the third terrain ladder in China, with abundant relic plants left over from quaternary glacier. As a rare plant gene bank in China, there are many national forest parks and natural reserves in this region. Abundant water and ore resources have made it one of the rarest eco-landscapes in China. Hence, the natural environment protection is of great importance to the construction of ecological civilization in Hubei province and even in China. China Western Development, water conservancy and hydropower projects, reservoir migration and other factors have exerted a profound impact on the ecological system of TGRA, leading to the increased risk of ecological degradation for a long time. Construction of the 180-m-tall dam was officially started in 1994. After the Three Gorges Reservoir impounding, the water level of dam has reached 135 m in 2003, 156 m in 2006, and 175 m in 2010. The construction of the Three Gorges Dam may have serious consequences for plant and animal species. Meanwhile, many positive implementations of policies and projects on vegetation protection promote the restoration for ecosystem structure and function of TGRA, such as Yangtze River protection forest engineering, natural forest protection project, and returning farmland to forest program.

2.2. Data Sources and Processing

2.2.1. Landscape Map

To obtain the landscape pattern information of the study area, three sets of remote sensing images (respectively obtained in1990, 2000 and 2010) need to be processed. Landsat-5 TM data with low cloud cover in summer time were selected as basic remote sensing sources. The Landsat-5 TM products with a spatial resolution of 30m are available from the United States Geological Survey (USGS) [35] and have been calibrated and atmospherically corrected for gas, aerosol, and cirrus-cloud effects. Image mosaic and clip were done according to the administrative boundaries of study area, and remote sensing images of the study area in1990, 2000 and 2010 were obtained.

The landscape was classified on the reference of Land Use Category System of the Chinese Academy of Sciences. Table 1 shows the landscape category system for use in our study, which is divided into 6 classes of the first class and 25 classes of the second class. Based on three sets of TM images, the landscape pattern information was extracted by a combination method of supervised classification and visual interpretation. To validate the accuracy of the landscape classification, 145 field points were sampled in June 2010. The field accuracy of first-order classification reaches 90%, and the second-order classification reaches 88%, which meet the research need.

Table 1. Landscape category system.

First Class	Second Class	First Class	Second Class
Farmland	Paddy field Dry land	Grassland	High coverage grassland Moderate coverage grassland Low coverage grassland
Woodland	Thick woodland Shrubbery land Sparse woodland Other woodland	Construction land	Urban land Rural residential land Industrial and traffic land
Waters	Canal Lake Reservoir or pond Permanent ice and snow Tideland Shoaly land	Unused land	Dene Gobi Saline and alkaline land Marshland Bare land Bare rock Other

2.2.2. Driving Factors

According to the status of the study area, both natural and human factors were selected to analyze driving forces for evolution of landscape pattern. Evaluation factors from two aspects of natural environment conditions and location were chose as internal driving forces, including DEM, slope, aspect, precipitation, temperature, distance to waters, distance to railway, distance to highway, distance to national road, distance to provincial road, distance to county road, distance to urban land and distance to residential land. As for external driving forces, population density and regional Gross Domestic Product (GDP) were selected from aspects of social and economic development.

DEM data was obtained from the ASTER Global Digital Elevation Model (ASTER GDEM) product, which is developed by the U.S. National Aeronautics and Space Administration (NASA) and Japan's Ministry of Economy, Trade, and Industry (METI). The ASTER GDEM covers land surfaces between 83° N and 83° S, and referenced to the 1984 World Geodetic System (WGS84)/1996 Earth Gravitational Model (EGM96) geoid. The product of ASTER GDEM Version 002 with spatial resolution of 30 m are available from Land Processes Distributed Active Archive Center (LP DAAC) of United States Geological Survey (USGS) [36]. The DEM data in 2010 of study region was processed and projected to an Albers equal area conic projection. Based on DEM data, slope and aspect map were created and extracted by using Slope and Aspect function of raster surface from 3D Analyst tools in ArcGIS 10.2.

The precipitation and temperature data were downloaded from the Meteorological Data Sharing Service System of China [37]. The annual average precipitation and air temperature data from 72 meteorological stations in 2010 that fully covered the entire region were selected. The annual precipitation and temperature were interpolated from a point to a regional scale using a kriging method with a spatial resolution of 30 m. Then, cross-validation was performed, and the interpolating error were approximately 76.67 mm and 0.68 degree which meet the accuracy requirements.

The spatial distribution of waters and construction land are all derived from the landscape map of the study area. The buffer analysis and assignment were done by distance function in Idrisi 17, and the buffer map of waters, traffic road at different level and town was drawn by setting 1.0 km buffer radius.

Night-time light data is a powerful tool to estimate socio-economic status as well as map gross domestic product (GDP) distribution and urban expansion [38,39]. The DMSP-OLS NTL composite has evolved into Version 4, containing global NTL time series 1992–2013. The composite for the year of 1992 and 2010 are available from the NOAA's NGDC [40]. Due to lack of data before 1992, the year composite data of 1992 was considered as night-time light data for the year of 1990. The stable light image, which has discarded ephemeral lights and background noise, from the composite was selected to reflect GDP status. The stable light images in 1990 and 2010 of study region was processed and projected to an Albers equal area conic projection.

Furthermore, population data at the level of community in 1990 and 2010 were collected from the fourth and sixth census of China respectively. Based on point data, Tyson polygons were constructed and the population density of each polygons was calculated. Then, the regional population density in 1990 and 2010 was obtained by interpolating points to a regional scale using an ordinary Kriging method with a spatial resolution of 30 m.

In the comprehensive evaluation of multiple factors, different factors often have different dimensions and dimensional units. To eliminate the effect of dimension, dimensionless treatment should be adopted before analysis. The data after dimensionless processing can accurately reflect the information contained in the original data. According to the research needs and data characteristics, equalization method in dimensionless treatment was used to reduce the loss of information in data and preserve differences in variation degree among factors. The equalization method follows that:

$$x_i' = \frac{x_i}{\overline{x_i}} \tag{1}$$

where, x_i is the original value of each factor, and $\overline{x_i}$ is the average value of all original value.

2.3. Methodology

There were four main steps in conducting this research. Figure 2 shows the details for each step. Firstly, the temporal and spatial variation characteristics of landscape pattern were analyzed by calculating the transition matrix of Markov model. Secondly, the habit quality was evaluated by using biodiversity module of InVEST model. Thirdly, the driving force for alterations in landscape pattern was analyzed. Finally, Ca-Markov model together with InVEST model were used to simulate future landscape pattern and habit quality in 2020 under different scenarios.

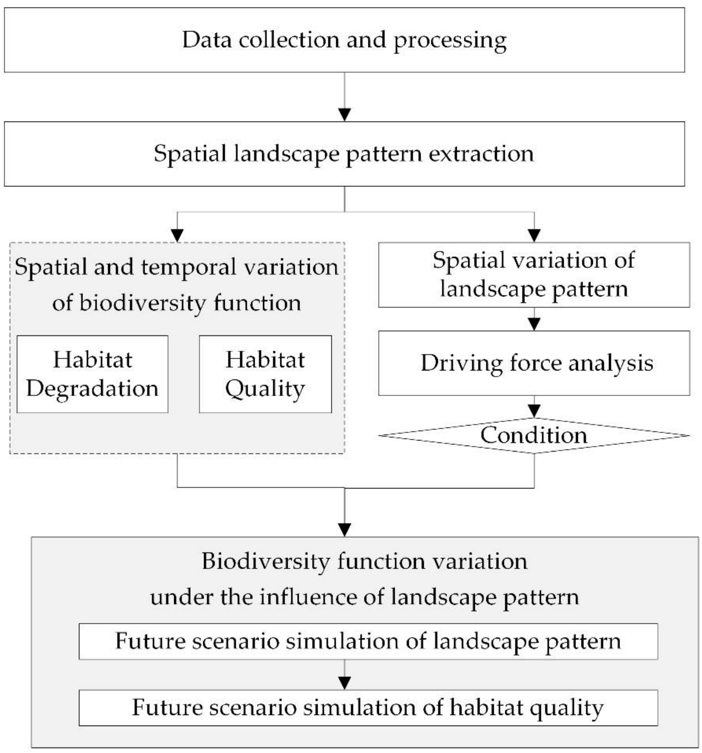

Figure 2. Flow chat for evolution and prediction of landscape pattern and biodiversity process.

2.3.1. Markov Chain

Markov chain is the simplest of stochastic models which is a transition matrix [41], and has been widely used for land cover change studies at various spatial scales [42]. In Markov model, the initial probability and the transition probabilities between different states are calculated, and the trend of landscape pattern changes over time is determined. Finally, the landscape pattern is predicted. Please note that the transition between landscape types is often non-directional, which means that the transition direction for the landscape types of current pixel allows for many possibilities in the next moment [43]. The transition probability of each landscape type is different, and the size of each possibilities are affected by many factors. The transition of landscape types is bi-directional, which not only transit from the current types into other types, but also from other types to the current types [44]. The types and quantity of landscape change constantly in the process of stochastic transition. The transition process of landscape types accords with the conditions of Markov's research, which is difficult to describe accurately by mathematical methods [45,46]. The output of Markov model is the probability of transition, P_{ij} is between state i and j. In a landscape with multiple land covers or land uses, the transition probability P_{ij} would be the probability that a landscape type (pixels) i in time t0 changes to landscape type j in time t1. As the transitions are probabilities, it follows that:

$$P = \begin{bmatrix} P_{11} & \cdots & P_{1n} \\ \vdots & \cdots & \vdots \\ P_{n1} & \cdots & P_{nn} \end{bmatrix} \tag{2}$$

where, n is number of landscape types, and Pij should meet two necessary conditions: $0 \leq P_{ij} \leq 1$; $\sum_{j=1}^{n} P_{ij} = 1$.

According to the principle of map algebra, the Markov transition matrix is established to quantitatively analyze the direction and intensity of the transition between different landscape types of second class. This transition matrix also can be used to predict the future landscape at time t2.

2.3.2. Habitat Quality

The biodiversity module in InVEST model maps the quality of habitat for a target conservation objective [47]. Landscape maps are converted into habitat maps by defining what landscape counts as habitat for various species [48]. Habitat quality is a function of the landscape type in a grid cell, the landscape in surrounding grid cells, and the sensitivity of the habitat in the grid cell to the threats posed by the surrounding landscape [49]. Landscape in surrounding grid cells can modify habitat quality in a grid cell. Each landscape type is given a habitat suitability or quality score of 0 to 1 for each particular measure of biodiversity with perfectly suitable habitat scored as 1 and non-habitat scored as 0 [50].

Sources of degradation were considered as those human modified landscape types (e.g., urban, agriculture, and roads) that cause edge effects [51,52]. Edge effects refer to changes in the biological and physical conditions that occur at a patch boundary and within adjacent patches (e.g., facilitating entry of predators, competitors, invasive species, toxic chemicals and other pollutants). The sensitivity of each habitat type to degradation is general principles of landscape ecology and conservation biology [53,54], and specific to each measure of biodiversity. The habitat quality was calculated combining landscape types information and threats of biodiversity, and the equation is shown in formula (3):

$$Q_{xj} = H_j \left(1 - \frac{{D_{xj}}^2}{{D_{xj}}^2 + k^2} \right) \tag{3}$$

where the quality of habitat in grid cell x that is in landscape type j be given by Q_{xj}. H_j represent the habitat suitability. Q_{xj} is equal to 0 if $H_j = 0$. Q_{xj} increases in H_j and decreases in D_{xj}. The k constant is the half-saturation constant and is set by the user. A grid cell's degradation score is translated into a habitat quality value using a half saturation function where the user determines the half-saturation value in InVEST model. The parameter k is equal to the D value where $1 - \frac{D_{xj}^2}{D_{xj}^2 + k^2} = 0.5$.

D_{xj} is the total threat level in grid cell x with landscape or habitat type j, and the equation is shown in formula (4):

$$D_{xj} = \sum_{r=1}^{R} \sum_{y=1}^{Y_r} \left(\omega_r / \sum_{r=1}^{R} \omega_r \right) r_y i_{rxy} \beta_x S_{jr} \tag{4}$$

where y indexes all grid cells on r's raster map and Y_r indicates the set of grid cells on r's raster map. S_{jr} is the sensitivity of habitat type j to threat r where values closer to 1 indicate greater sensitivity. Please note that each threat map can have a unique number of grid cells due to variation in raster resolution If $S_{jr} = 0$ then D_{xj} is not a function of threat r. Also note that threat weights are normalized so that the sum across all threats weights equals 1.

The impact of threat r that originates in grid cell y, r_y, on habitat in grid cell x is given by i_{rxy} and is represented by the following equations,

$$i_{rxy} = 1 - \left(\frac{d_{xy}}{d_{r\ max}} \right) \quad if\ linear \tag{5}$$

$$i_{rxy} = \ exp\left(-\left(\frac{2.99}{d_{r\ max}} \right) d_{xy} \right) \ if\ exponential \tag{6}$$

where d_{xy} is the linear distance between grid cells x and y and $d_{r\ max}$ is the maximum effective distance of threat r's reach across space. For example, if an exponential decline is selected and the maximum impact distance of a threat is set at 1 km, the impact of the threat on a grid cell's habitat will decline by ~50% when the grid cell is 200 m from r's source. If $i_{rxy} > 0$ then grid cell x is in degradation source r_y's disturbance zone. ω_r is the threat weight. β_x indicates the level of accessibility in grid cell x where 1 indicates complete accessibility.

Some input parameters in model were determined from the literatures [32,49] and 12 experts, who are all in the field of regional ecological assessment and environmental simulation from the key research and development project of typical vulnerable ecological restoration and protection in China. The following parameters were input into the model, including landscape maps (three periods), threats factor layers (including paddy field, dry land, urban land, rural resident land, industrial and traffic land and bare land), index of threats and sensitivity (Table 2), weight of threat factor (Table 3), sensitivity of landscape types to each threat, and accessibility to threats, and half-saturation constant. The habitat quality maps were obtained after running the biodiversity module, and the grid resolution was set to 30 m according to remote sensing data requirements. Habitat quality scores should be interpreted as relative scores with higher scores indicating landscapes more favorable for the given conservation objective. The score of landscape habitat quality cannot be interpreted as a prediction of species persistence on the landscape or other direct measure of species conservation. The InVEST habitat model does not convert habitat quality measures into monetary values.

Table 2. Landscape types and its sensitivity to each threat.

Landscape Types	Habitat	Paddy Fields	Dry Land	Urban Land	Rural Resident Land	Industrial and Traffic Land	Bare Land
Paddy field	0	0	1	0	0	0.5	0.4
Dry land	0	1	0	0	0	0.5	0.4
Thick woodland	1	1	1	0.2	0.2	0.3	0.3
Shrubbery land	1	0.5	0.5	0.2	0.2	0.2	0.1
Sparse woodland	1	0.7	0.9	0.2	0.8	0.4	0.8
Other woodland	1	0.5	0.5	0.2	0.2	0	0
High coverage grassland	0.5	0.8	0.8	0.4	0.7	0.4	0.4
Moderate coverage grassland	1	0.5	0.5	0.2	0.2	0	0

Table 2. *Cont.*

Landscape Types	Habitat	Paddy Fields	Dry Land	Urban Land	Rural Resident Land	Industrial and Traffic Land	Bare Land
Low coverage grassland	1	0.8	0.8	0	0	0.4	0.4
Canal	0	0.3	0.3	0.3	0.3	0.8	0.2
Lake	1	0.5	0.4	0	0	0.4	0.4
Reservoir or pond	1	0	1	0.7	0.4	0.4	0.6
Shoaly land	1	0.8	0.8	0	0	0.4	0.4
Urban land	0	0	0	0	0	0.8	0.7
Rural residential land	0.6	0.2	0.2	0	0	0	0.8
Industrial and traffic land	0.7	0.2	0.2	0	0	0	0.8
Bare land	0.5	0.2	0.2	0	0	0	0.8

Table 3. Attributes of threat data.

Threat	Maximum Effective Distance (km)	Weight	DECAY
Paddy fields	0.5	0.5	Exponential
Dry land	0.5	0.5	Exponential
Urban land	3	0.7	Exponential
Rural residential land	2	0.7	Exponential
Industrial and traffic land	8	1	Linear
Bare land	10	0.3	Exponential

2.3.3. Logistic Regression Model

Logistic Regression (LR) model is a nonlinear model, forming a multivariate regression relation between a dependent variable and a set of independent variables [55,56]. The principle of LR rests on the analysis of a problem, in which a result measured with dichotomous variables such as 0 and 1 or true and false, is determined from one or more independent factors [57]. The goal of LR is to find the best fitting (yet reasonable) model to describe the relationship between a dependent variable (the presence or absence of event) and a set of independent variables [58,59]. Compared with linear regression analysis models, the advantage of LR is that the variables may be either continuous or discrete, the value of variable can be any value in the real number range, and they do not necessarily follow normal distributions. Maximum likelihood estimation is used in the algorithm of LR model after transforming the dependent variable into a logit variable [55,60]. Logistic regression has been widely applied for driving force analysis by many researchers [58–63], which can generate the regression relation with dichotomous variables such as 0 and 1 or true and false [64]. The equation of LR model follows (7):

$$Y = \lg\left(\frac{P_i}{1-P_i}\right) = \mathrm{logit}(P_i) = \propto +\beta_1 X_1 + \beta_2 X_2 + \cdots + \beta_n X_n \tag{7}$$

$$P_i = \frac{e^y}{1+e^y} \tag{8}$$

where, P_i is the probability that a certain landscape type i may appear or disappear in each grid. Function Y is represented as $\mathrm{logit}(P_i)$, i.e., the log (to base e) of the odds or likelihood ratio that the dependent variable. X_n denotes each influencing factor. $\propto$ represents the constant term. $\beta_1, \beta_2, \cdots, \beta_n$ are the partial regression coefficient of LR model, representing the impact of the independent variable X_n on Y. When the coefficient is positive and statistically significant, which means that the event of Y event is more likely to occur as the value of corresponding independent variables increases under the control of other independent variables. When the coefficient is negative and statistically significant, which means that the odds of the event Y occurring decreases as the value of corresponding independent variables increases under the control of other independent variables. A coefficient of 0 does not change the odds one way or another.

In this study, LR establishes a functional relationship between the binary coded landscape locations (presence or absence of a landscape) and different factors that are recognized as playing a role in landscape development. For each landscape type, when the landscape type is changed, its value is set as Y = 1; otherwise, Y = 0. LR generates the model statistics and coefficients of a formula useful to describe the relationship between the binary coded landscape locations (presence or absence of a landscape) and different factors. Relative Operating Characteristics (ROC) is usually used to test the regression effect [65].

LR model estimates the probability of a certain event occurring, therefore, selecting influencing factors that have a significant impact on the landscape pattern, and determining the quantitative relationship between them. According to the status of the study area, both natural and human factors were selected to construct the index system of driving forces for landscape evolution, and each factor was spatialized. Before the analyzing work of LR model, it is necessary to normalize the data of different measuring scales. The results should be interpreted with caution if the data fail to normalized in a manner LR model needs. In the application for exploring influencing factors on landscape variation, the common solution is to create layers of binary values for each class of an independent parameter [59,66,67]. Here, we used binary landscape data (when the landscape type is changed, its value is 1; otherwise, 0.) from all over the area. Then, the driving mechanism of landscape evolution from 1990 to 2010 can be explored by using LR model.

2.3.4. CA-Markov Model

CA-Markov model consists of Markov chain and Cellular Automata (CA) model. As a method of studying nonlinear science, CA model is a spatially dynamic model, whose time, space and state are discrete. CA model consists of four parts, including cellular and its state, cellular space, cellular neighborhood and transition rules. In cellular space, every cell has its limited and particular state, and will be update according to the defined local rules. The interaction of these local rules forms a dynamic evolution system. In a CA model, the transition of a cell from one landscape to another depends on the state of the neighborhood cells [68]. A cell will have a higher probability to transit to land-use type 'A' than to a land-use type 'B' if the cell is in closer proximity to land-use type 'A'. Thus, the CA model not only uses the information of the previous state of a landscape type as done by a Markov model but also uses the state of neighborhood cells for its transition rules.

CA model has been widely used for land use and land cover (LULC) change analysis, which can be expressed by the following formula:

$$S_{(t+1)} = f\left(S_{(t)}, N\right) \tag{9}$$

where, S is the set of finite and discrete cellular states, t and $t+1$ represent different moment in time, N is cellular neighborhood, and f is the cellular transition rules in local space.

CA model adds spatial character to a Markov model, thus combining CA-Markov model. In CA-Markov model, each landscape pixel is a cellular, and the landscape type of each cellular refers to a cellular state. With the support of GIS software, the transition of cellular state is determined by calculating the transition area matrix and conditional transition probability maps, and the change of landscape pattern is simulated [23]. CA-Markov module of IDRISI 17 was used to predict future landscape. The specific implementation process is as follows:

In the first step, a Markov model is run using the landscape maps of different period to predict for future. In doing so, the CA Markov model makes the assumption that the driving factors affecting change in all time periods are same. The outputs of this step are a transition area matrix, a transition probability matrix and a series of transition probability maps (probability of each pixel to each landscape types).

In the second step, CA analysis is run using the landscape maps and outputs from the Markov module, i.e., transition area matrix, transition probability maps and contiguity. The combined cellular automata and Markov chain method of the CA Markov module adds an element of spatial contiguity as well as knowledge of the likely spatial distribution of transitions to Markov chain analysis. The inherent suitability of each pixel and the restriction factors for each landscape types are established. The inherent suitability of each pixel is obtained by using the transition probability maps in an iterative process of CA Markov module. It is considered that within a certain threshold value, the suitability is the highest, which is set for 1. When exceeding the threshold, the Sigmoid function decreases with the distance until the extremely unsuitable distance is reached, and the adaptability is set for 0. After exceeding this distance, the suitability will not change. Next, an Analytic Hierarchy Process (AHP) method is used to weight sum the suitability layers the results of LR analysis. Then, OWA aggregation is done by selecting Location 4. In addition, the restriction factors obtained by LR analysis also were selected to put in model.

In the third step, the start time and the number of CA cycles were determined. One year represents one iteration, the iteration is taken as 10. For our present study, the time period of 1990 and 2000 should be used as reference map for validating the corresponding dates predicted maps of 2010, because the data were not used to build the respective models. If the predicted 2010 map is similar to reference 2010 map, we considered that the model performed well.

In the final step, validation was done simply by cross tabulating the predicted and observed landscape map of respective years. In present study, the predicted landscape map of 2010 was used to compare with reference 2010 map. The Kappa index was used to test the prediction accuracy of model, which can be expressed by the following formula:

$$\mathrm{Kappa} = (\mathrm{P}_0 - \mathrm{P}_\mathrm{c})/(\mathrm{P}_0 + \mathrm{P}_\mathrm{c}) \quad (10)$$

where P_0 is the correct ratio of simulation, P_c is the correct ratio of random simulation, and P_p is the correct ratio of ideal classification.

3. Results

3.1. Spatial Landscape Pattern Analysis

Woodland, farmland and grassland are the main landscape types in the study area, accounting for 95% of the total area, of which 75% is woodland (Figure 3). From 1990 to 2010, the landscape pattern of the study area has changed slightly (Figure 4). Among the landscape types, woodland, waters and construction land had the greatest change in proportion. The area of woodland, farmland and grassland has been decreasing gradually, and the area of waters and construction land increased in the past two decades. The area of unused land slightly declined. The area of woodland, farmland and grassland in 1990 were 9631.88 km^2, 1598.50 km^2 and 815.38 km^2. By 2010, the area of above landscape types was 9539.11 km^2, 1579.64 km^2 and 813.85 km^2 respectively. The area of waters and construction land in 1990 were 131.02 km^2 and 67.71 km^2, and the area of above landscape types was 190.50 km^2 and 121.51 km^2 in 2010. These landscape variations fit the facts of the Three Gorges Dam construction, impoundment of the Three Gorges Reservoir, immigration and expansion of construction land in study area.

Figure 5 exhibits the landscape transition map from 1990 to 2010 by overlaying landscape maps of before and after periods. The landscape transition matrix was statistically sorted. The results showed that 98.62% of the landscape types did not change within 20 years, and only about 1.38% of the landscape types changed (Table 4). The most varied landscape types were woodland, farmland, waters and construction land. The land occupancy of Three Gorge Dam construction and the impoundment of TGR could be the reason for the decreasing area of woodland and farmland located with the average elevation of 140 m. The increasing area of waters and construction land could be explained by the impoundment of TGR, migration and resettlement, and urbanization.

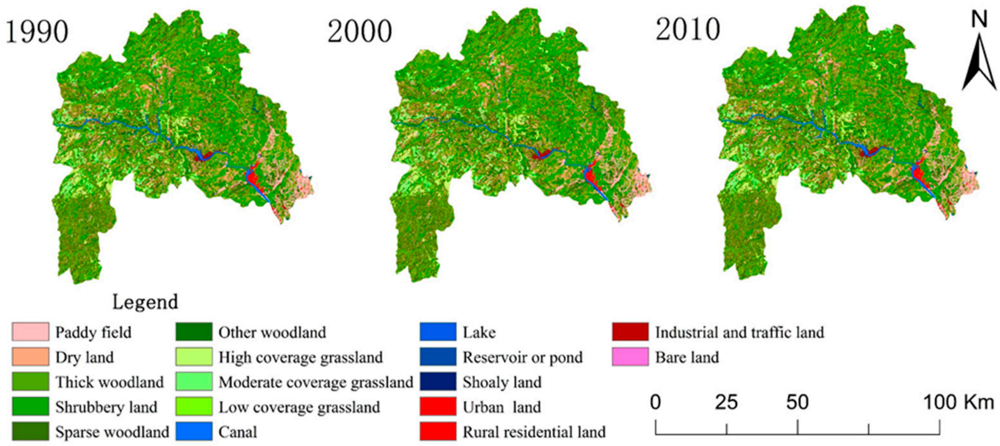

Figure 3. Spatial distribution maps of landscape in 1990, 2000, 2010.

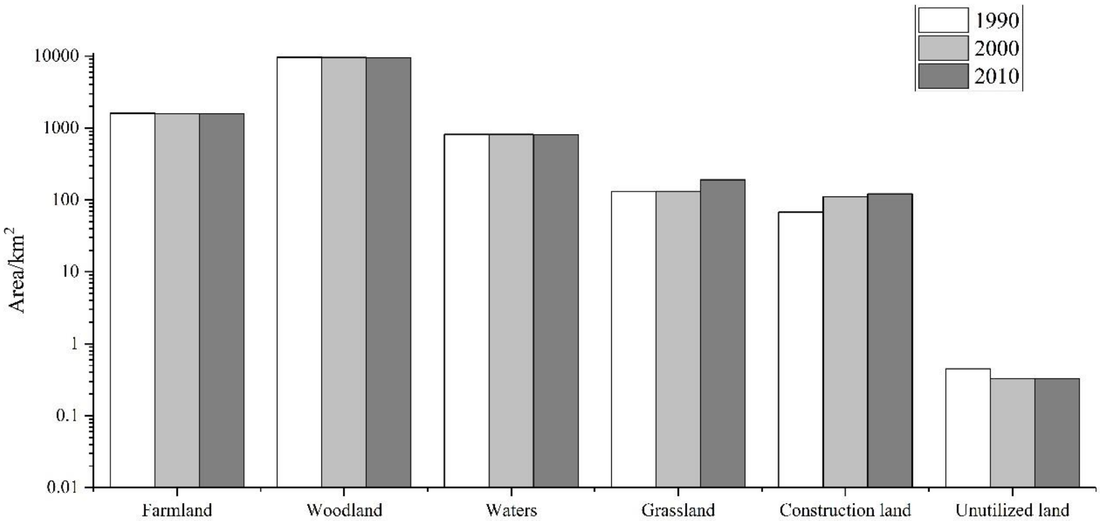

Figure 4. Landscape area of first class in 1990, 2000 and 2010.

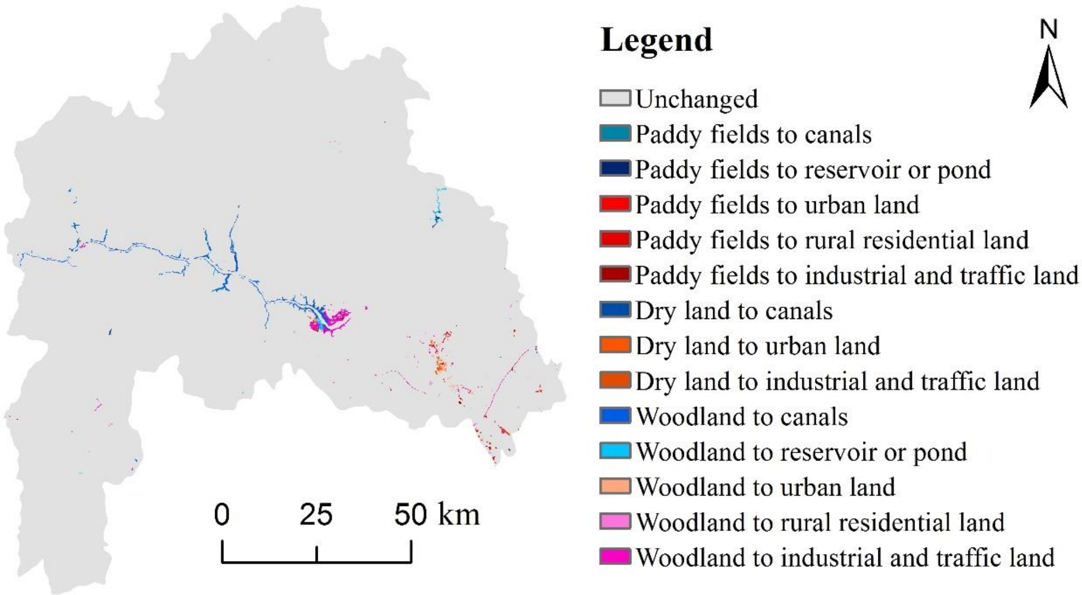

Figure 5. Spatial variation map of landscape pattern between 1990 and 2010.

Figure 6 illustrates the transfer in and out rate of landscape types. From 1990 to 2010, shoaly land and unused land had relatively high transfer-out rate, with a decreasing ratio of 41.86% and 27.05% respectively. Most of shoaly land mainly transferred into canal and reservoir or pond. Unused land mainly transferred into urban land, industrial and traffic land. Waters (canal, lake, reservoir or pond) and industrial and traffic land had relatively high transfer-in rate. Industrial and traffic land has highest transfer-in rate. The area of industrial and traffic land in 2010 was six times bigger than in 1990, and they were mainly transferred from woodland and farmland. Lake has the second-highest transfer-in rate with an increasing ratio of 136.36%, mainly transferring from woodland.

In the whole study area, waters and construction land have been the most dramatic changed landscape types. These variations mainly concentrated in main urban areas of Yichang city, extending downstream along the Yangtze River. Some of the variation located in Badong County. The expansion of waters was distributed around Three Gorges dam site in Zigui County and along the main and tributary banks of the Yangtze River. The strong increasing trend of construction land could be explained by the continuous improvement of settlement scale, the demand for supporting and improving facilities after three periods of immigration of the pilot project.

Table 4. Statistics information of main landscape changing types from 1990 to 2010 (km^2, %)

Changed Type	Area	Percentage
Unchanged	12,067.19	98.62
Woodland to canals	41.52	0.34
Woodland to industrial and traffic land	26.21	0.22
Woodland to reservoir or pond	8.23	0.07
Woodland to urban land	6.84	0.06
Paddy fields to canal	3.82	0.03
Paddy field to industrial and traffic land	3.77	0.03
Paddy fields to urban land	3.43	0.03
Dry land to urban land	3.31	0.03
Dry land to industrial and traffic land	3.28	0.03
Dry land to canals	2.95	0.02
Woodland to rural residential land	2.90	0.02
Paddy fields to reservoir or pond	2.51	0.02
Paddy fields to rural residential land	2.32	0.02

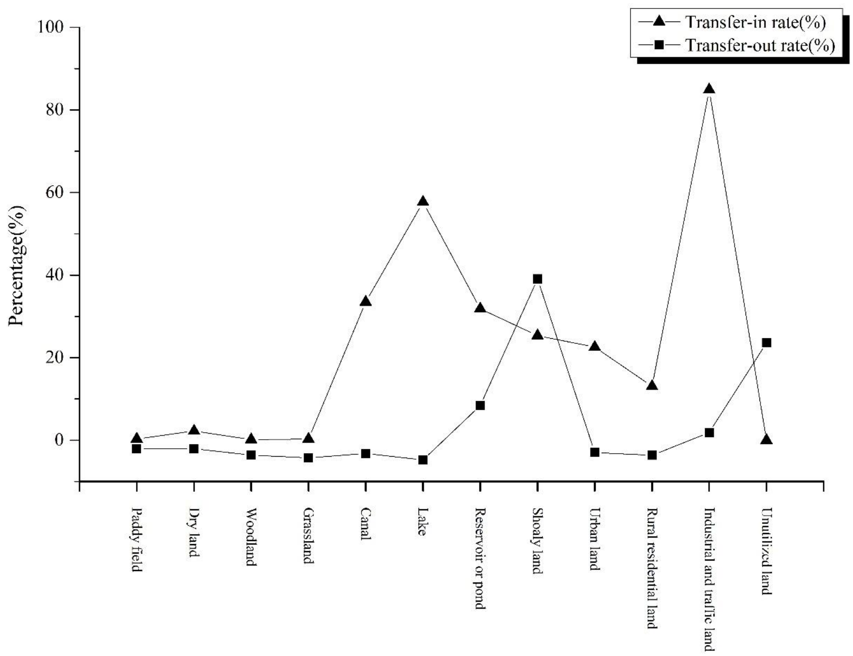

Figure 6. Transfer rate of landscape types between 1990 and 2010.

3.2. Spatial and Temporal Variation of Biodiversity

3.2.1. Analysis of Habitat Degradation

The value of habitat degradation index ranging from 0 to 1 represents the relative habitat degradation level of the current landscape, where 1 denotes high degradation and 0 denotes low degradation. Figure 7 shows the spatial distribution map of habitat degradation. The maximum value of habitat degradation index were 0.1188, 0.1194 and 0.1195 respectively, showing a gradually increasing trend from 1990 to 2010. In terms of spatial pattern, the areas with higher habitat degradation index were mainly distributed in main urban areas of Yichang city, southeastern parts of Yiling districts and south-central parts of Xingshan county, and the corresponding landscape types were urban land, rural residential land and canal. The areas with relatively low habitat degradation index were mainly distributed in the central and southwest of study area, such as Zigui county and Badong county, and the corresponding landscape type was woodland. Overall, the TGR area (Hubei section) developed rapidly from 1990 to 2010, causing a causing a continuously increasing trend of habitat degradation.

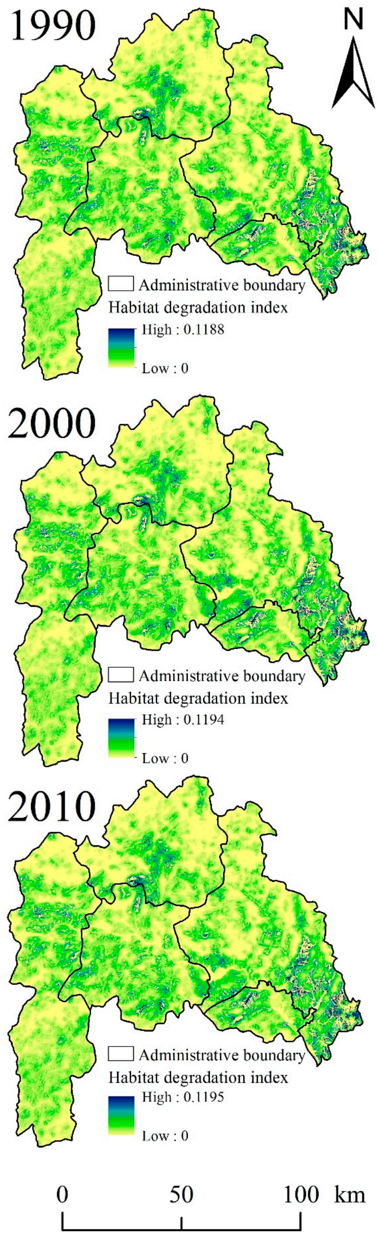

Figure 7. Spatial distribution pattern of habitat degradation index in 1990, 2000, 2010.

3.2.2. Analysis of Habitat Quality

Higher values indicate better habitat quality vis-a-vis the distribution of habitat quality across the rest of the landscape. To facilitate the observation of changes in habitat quality, the division method of natural breaks was adopted to assign grades according to the output values of habitat quality. The habitat quality was divided into five grades, they are low, relatively low, medium, relatively high, and high, and these grades are on behalf of poor habitat quality, relatively poor habitat quality, medium habitat quality, relatively high habitat quality, and high habitat quality respectively (Table 5).

Table 5. Classification value of habitat quality in study area

Grade	Value Range	Description
Low	0~0.1	Poor habitat quality
Relatively low	0.1~0.6	Relatively poor habitat quality
Medium	0.6~0.8	Medium habitat quality
Relatively high	0.8~0.9	Relatively high habitat quality
High	0.9~1	High habitat quality

Based on divisions, the spatial distribution map of habitat quality grade in three phases was obtained (Figure 8), and the variations of habitat quality were statistically analyzed (Table 6). Overall, woodland, farmland and grassland occupied for 95% of the total area, thus the habitat quality of whole area was at a relatively high grade. The areas with high habitat quality grade was mainly distributed in Badang, Zigui and Xingshan county where the coverage of woodland. The areas with low habitat quality grade was mainly distributed in main urban areas of Yichang city, southeastern parts of Yiling districts, southern parts of Xingshan county and shoaly areas along the banks of the Yangtze River, where the corresponding landscape types are construction land and canals with higher elevation.

The overall habitat quality score declined slightly from 1990 to 2010. Habitat quality achieved a score of 0.8653 in 1990, 0.8259 in 2000 and 0.8155 in 2010. Most of areas was in a relatively high grade of habitat quality, the overall score of habitat quality decreased over the past twenty years. The magnitude of the declines for overall habitat quality was likely to be slight, but obvious in some local areas. The area of landscape with high habitat quality grade decreased obviously. The area of landscape with low and relatively low habitat quality grade increased. In 1990, the areas with high grade of habitat quality occupied for 84.78% of the total area, and accounted for 84.02% in 2010 with a decline area of 0.76%. The area of low and relatively low habitat quality grade increased by 0.3% and 0.44% respectively.

The overall habitat quality continues to decrease and the urbanization process continues to develop combining with the analysis of the habitat degradation. From 1990 to 2010, the overall fluctuation of habitat quality was relatively small, and the variation areas mainly were distributed in urban areas, canal areas with higher elevation and areas along the banks of the Yangtze River. In general, the fluctuation of habitat quality tended to be stable as a whole.

Based on habitat quality maps of 1990 and 2010, spatial changes of habitat quality were obtained in the past two decades (Figure 9). The landscape transition showed a decreasing trend of habitat quality grade from high to low and relatively low grade in areas of study region. The changes of habitat quality grade from high to low grade were that large areas of woodland and grassland have been developed for residential land, industrial and traffic land. The changes of habitat quality grade from high to relatively low grade were the transitions from woodland and grassland to canals. The construction of the Three Gorges Dam, impoundment in the TGR area and environmental migration contributed the increasing area of construction land and waters, decreasing area of woodland and grassland, and a decline of habitat quality as a whole.

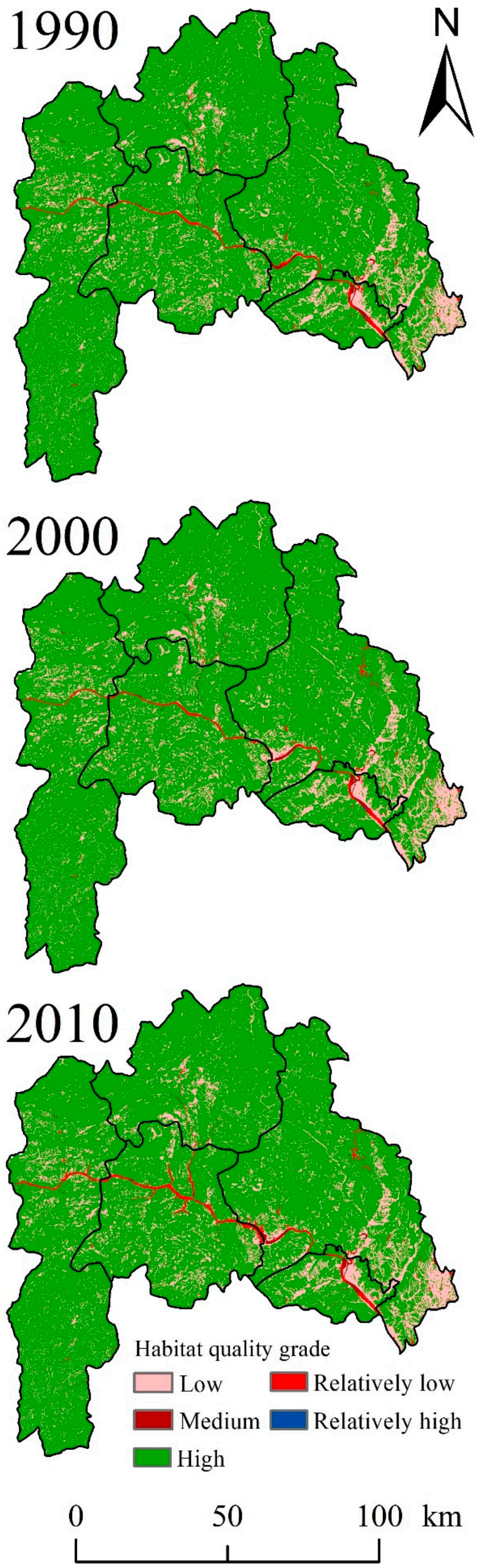

Figure 8. Spatial distribution pattern of habitat quality in 1990, 2000, 2010.

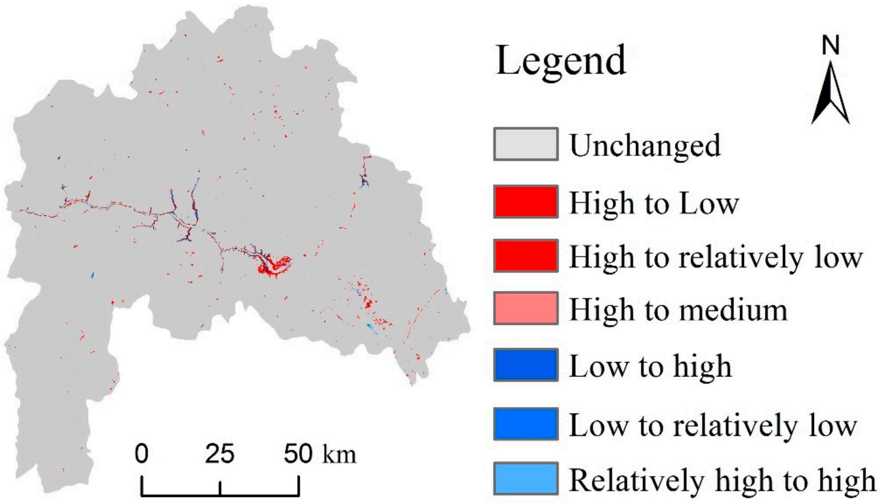

Figure 9. Spatial variation map of habitat quality between 1990 and 2010.

Table 6. Area and percentage of habitat quality at all grades (km^2, %)

Grade	1990		2000		2010		1990 to 2010	
	Area	Percentage	Area	Percentage	Area	Percentage	Area	Percentage
Low	1664.66	13.60	1707.71	13.95	1701.48	13.90	36.81	0.30
Relatively low	100.28	0.82	99.53	0.81	153.90	1.26	53.62	0.44
Medium	30.18	0.25	32.14	0.26	36.27	0.30	6.08	0.05
Relatively high	68.45	0.56	67.83	0.55	65.39	0.53	−3.06	−0.03
High	10,379.36	84.78	10,337.74	84.42	10,287.91	84.02	−91.45	−0.76

3.3. Driving Force for Spatial Variation of Landscape Pattern

With the construction of Dam, impoundment and reservoir resettlement in the TGR area, the landscape pattern has been changed, leading to the decline of habitat quality. According to statistics of landscape pattern, the most varied landscape types were woodland, farmland, waters and construction land. Hence, both natural factors and human factors were selected to explore the driving mechanism of spatial variation of landscape pattern. To investigate the most dominant influencing factors, the following 15 factors are listed, including Night-time light (X_1), population density (X_2), DEM (X_3), slope (X_4), aspect (X_5), precipitation (X_6), temperature (X_7), distance to waters (X_8), distance to railway (X_9), distance to highway (X_{10}), distance to national road (X_{11}), distance to provincial road (X_{12}), distance to county road (X_{13}), distance to urban land (X_{14}), and distance to rural residential land (X_{15}). Table 7 shows the results of LR analysis.

Table 7. Results of Logistic regression analysis.

Independent Parameter	Paddy Field	Dry Land	Woodland	Grassland	Canal	Lake	Reservoir or Pond	Shoaly Land	Urban Land	Rural Residential Land	Industrial and Traffic Land	Bare Land
Intercept	−4.30	−2.62	−2.34	−0.11	17.70	−161.50	1.29	−18.74	−378.72	−37.42	−28.93	−1136.34
X_1	−0.79	0.44	0.40	84.61	543.06	2.21	−0.64	2.15	7.13	827.33	0.00	392.10
X_2	−0.49	−0.40	−0.84	−0.38	−0.05	6.94	1.23	−0.38	−1.35	1.52	−2.09	4.08
X_3	−58.21	−4.04	−32.79	4.45	−369	−368.32	102.37	202.56	124.07	9.55	−74.06	478.59
X_4	71.12	7.93	48.93	3.81	428.69	480.34	−130.03	−193.84	−11.88	316.47	71.66	−705.36
X_5	2.60	1.08	−5.16	−10.89	−17.26	−74.72	23.38	−8.73	−23.62	−9.02	21.00	−24.43
X_6	1.80	−13.27	−12.43	−40.05	−300	1757.60	87.07	−161.30	−1079.92	483.07	298.85	16,293.71
X_7	−1.70	16.32	15.94	48.65	363.17	−2082	−87.57	159.51	467,520	−587.76	−362.09	−19725
X_8	0.10	0.03	−0.08	0.00	−0.73	7.65	−0.59	−0.15	−1.05	0.81	0.33	−5.64
X_9	0.00	−0.01	0.04	−0.02	0.13	0.00	−0.12	0.10	−0.06	0.37	0.02	−12.95
X_{10}	0.07	0.02	0.07	0.13	0.35	−1.82	0.06	−0.02	−1.04	−0.39	−0.79	−9.33
X_{11}	0.04	0.02	0.12	0.00	0.30	0.05	0.11	0.06	−0.10	0.36	0.34	12.06
X_{12}	0.01	0.02	−0.12	−0.03	0.33	4.41	0.20	−0.44	2.00	1.07	−0.25	43.52
X_{13}	−0.44	−0.18	−0.37	−0.39	0.35	8.53	−0.44	0.02	0.28	1.21	−2.23	23.70
X_{14}	−0.07	−0.07	−0.14	−0.08	−0.51	−7.18	0.22	0.03	−192.14	−0.97	−0.08	−105.56
X_{15}	0.21	−0.06	0.04	−0.12	0.53	−2.62	0.55	0.06	−1.40	−349.51	0.33	9.22
ROC	0.94	0.83	0.92	0.86	0.99	0.85	0.95	0.98	0.90	0.88	0.98	0.87

The results of correlation analysis denoted that, compared with human factors, natural factors played a more important role in the spatial variation of each landscape types. From 1990 to 2010, the most influencing factors were DEM, slope, precipitation and temperature. The mean value of ROC reached 0.91, and the ROC value of each type was more than 0.8, indicating the good performance of LR model in analyzing the driving factors of landscape pattern variation.

For spatial variation of farmland, the average ROC value was 0.88. DEM, slope and temperature had the relatively high correlation value, which means that these three factors were the crucial determinants for spatial evolution of farmland. For spatial variation of dryland, precipitation and temperature were considered special factors. For spatial variation of paddy field, DEM and slope were the most important explanatory variables. The occurrence of paddy fields is often closely correlated with terrain. The exits of lower elevation and gentle slope greatly impact the occurrence of paddy field.

For spatial variation of woodland, the average ROC value was 0.92. DEM, slope, temperature and precipitation had the relatively high correlation value, illustrating that climate and terrain restricted the occurrence of woodland.

For spatial variation of grassland, the average ROC value was 0.86. Nighttime light, temperature and precipitation had the relatively high correlation value, indicating that human activities and climate affected the presence or absence of grassland. Among them, nighttime light had the highest correlation value, illustrating that the intensification of human economic activities leads to the transition of grassland to artificial surface.

For spatial variation of waters, the average ROC value was 0.94. DEM, slope, temperature and precipitation had the relatively high correlation value. Specially, the coefficient that belongs to the variable nighttime light strongly departs from 0 and led to the inference that human economic activities has a higher effect on the development of canal than any other variable. Along with the increasing activities of human beings, the demand for canal increased as well as the awareness of canal conservation. Terrain and climate were the dominant explanatory variables for the occurrence of lake, reservoir or pond, and shoal land. There were significant negative correlations between the development of those waters and elevation, which concluded that the higher elevation, the less probability of occurrence of lake, reservoir or pond, and shoal land would be. Those waters mainly occurred in relatively gentle terrain, and has significant correlation with precipitation and temperature.

For occurrence of construction land, the average ROC value was 0.92. DEM, temperature and precipitation, and nighttime light showed the relatively high correlation value. Terrain, climate and human economic activities were the dominant explanatory variables for the occurrence of construction land. For development of urban land, temperature and precipitation had relatively high correlation value, which indicated that climate has a higher effect on the development of urban land. For development of rural residential land, nighttime light had the highest correlation value. The impact of nighttime light variation on the occurrence of rural residential land was quite remarkable. Frequent and intensive human activities have caused increasing rural residential areas. For occurrence of industrial and traffic land, DEM had highest correlation value, which concluded that the lower elevation, the more likely the occurrence of industrial and traffic land would cause.

For occurrence of bare land, the ROC value was 0.87. Nighttime light, DEM, Slope, temperature, precipitation and distance to urban land had relatively high correlation value, illustrating that human activities, terrain, and climate all affected the occurrence of bare land. As human activities intensified, there will be a certain damage to vegetation, thus leading to the increasing probability of occurrence of bare land.

Although natural factors were highly correlated with presence or absence of landscape, they were not the crucial factors to drive the evolution of landscape distribution. Natural factors (e.g., Terrain and climate) evolve relatively slow, and usually will not change much in a shorter period (<20 years). To a certain extent, the driving force of socio-economic factors plays a role in evolution of landscape pattern, which cannot be neglected. The rapid development of central China brings out the economic rise in recent years, which can be reflected through the changes of nighttime light data. In our study, changes in nighttime light data, as a restriction input factor, was selected to add into the forecast model of landscape pattern, thus the potential evolution direction could be predicted.

3.4. Biodiversity Variation under the Influence of Landscape Pattern

In this section, CA-Markov model was used to adjust the future landscape pattern under different scenarios. Based on simulated landscape patterns, future habitat quality maps were evaluated through InVEST model. Therefore, the impact of landscape pattern dynamics on biodiversity was evaluated.

3.4.1. Forecast of Landscape Pattern

To verify the accuracy of the prediction, the observed and predicted landscape map of 2010 were input into CROSSTAB module in IDRISI. The Kappa coefficient reached 0.89, which showed the well performance of prediction model. Using the validated CA-Markov models will therefore allow us to predict the landscape map of 2020 under the business as usual and the ecological protection scenario.

Under the business as usual scenario, the landscape pattern will not be affected by policy adjustments, and it would change according to the transition probability matrix of each landscape types from 2000 to 2010. In addition, nighttime light together with other restriction factors were used to put into CA-Markov model. Figure 10a exhibits the landscape distribution map of 2020 under the business as usual scenario. By 2020, the variation trend of landscape pattern was basically consistent with the previous decades (Figure 11). The area of farmland, woodland and grassland reduced continuously, and the area of construction land increased continuously. The urban land has the largest changing rate among all the landscape types, with a changing rate of 19.05% from 2010 to 2020. The area of urban land increases rapidly, reaching an area of 60.97 km^2 by 2020. The area of canal has decreased to a certain extent, with a changing rate of 3.25%. Following this business as usual growth pattern, the area of construction land will continue to grow rapidly, and the regional ecological security will be endangered, which is no longer sustainable.

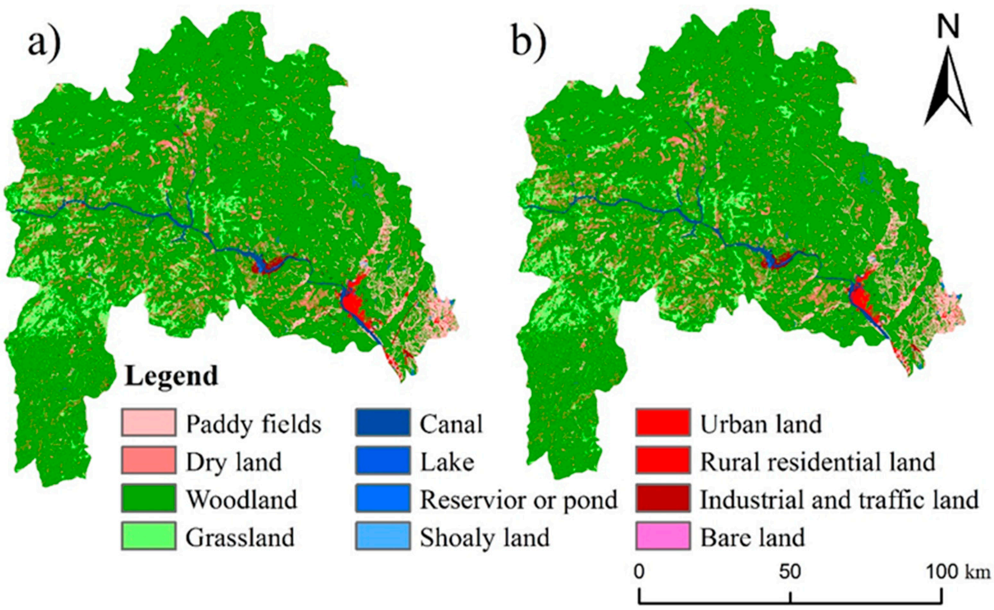

Figure 10. Forecast maps of landscape in 2020 under (**a**) Business as usual scenario and (**b**) Ecological protection scenario.

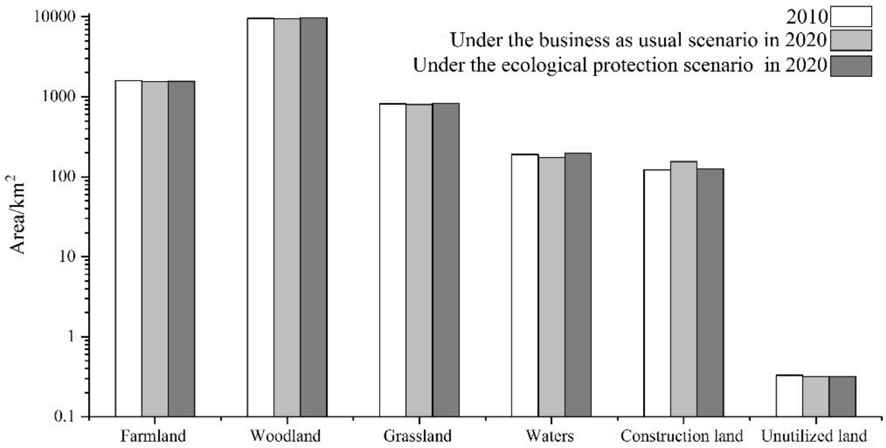

Figure 11. The comparison of landscape area at first class in 2010, under business as usual scenario and ecological protection scenario in 2020.

Under the ecological protection scenario, the area of woodland and waters were strictly protected, and the transition of farmland and construction land into above two landscape types was required to strengthen. The transition setting was as follows: the transition probability from farmland and woodland to construction land reduced by 3% and 1% respectively, from waters to construction land decreased by 2%, and from farmland to woodland increased by 1%. Figure 10b illustrates the simulated landscape map of 2020 under the ecological protection scenario. By 2020, the variation trend of landscape pattern was quite different from the previous decades, showing a decreasing area of farmland, increasing area of woodland and grassland, and relatively constant area of waters (Figure 11). Grassland has the largest changing rate among all the landscape types, with a changing rate of 17.72% from 2010 to 2020. The area of grassland reached 957.87 km^2. The area of urban land increases slightly, with a changing rate of 3.42% and reaching an area of 52.97 km^2 by 2020. The area of shoaly land has decreased sharply, with a changing rate of 16.12%. Following this ecological protection pattern, the quality habitat will increase to the 2000's level and the natural environment will improve, leading to harmonious development between human and nature.

3.4.2. Prediction of Habitat Quality

Based on predicted landscape maps, the habitat quality maps under business as usual scenario and ecological protection scenario were obtained using InVEST model, and the variations of habitat quality were statistically analyzed.

Figure 12 exhibits the future habitat quality map under the business as usual scenario. The variation trend of habitat quality in this scenario was consistent with the previous decades. The overall habitat quality score declined slightly, with an increasing area of low habitat quality in some local regions (Table 8). Habitat quality achieved a score of 0.8051 in 2020, and declined by 0.0104 when compared with 2010. The area of landscape with low habitat quality grade continuously increased and the area of landscape with medium and above habitat quality grade continuously decreased. The areas with relatively low and low grade of habitat quality occupied for 15.30% of the total area, with an increasing rate of 0.14% when compared with 2010. From 2010 to 2020, the transition of landscape pattern from high to low habitat quality grade occurred in some parts of the study area, and most of areas with low-grade habitat quality were construction land. The main change process of high-grade habitat quality was that large area of woodland and grassland was developed for construction land, which concentrated in main urban areas of Yichang city, southeastern parts of Yiling districts and northern parts of Xingshan county. The increasing urbanization and the construction of industrial and traffic land, decreasing of woodland and grassland would contribute the continuously decline of habitat quality as a whole.

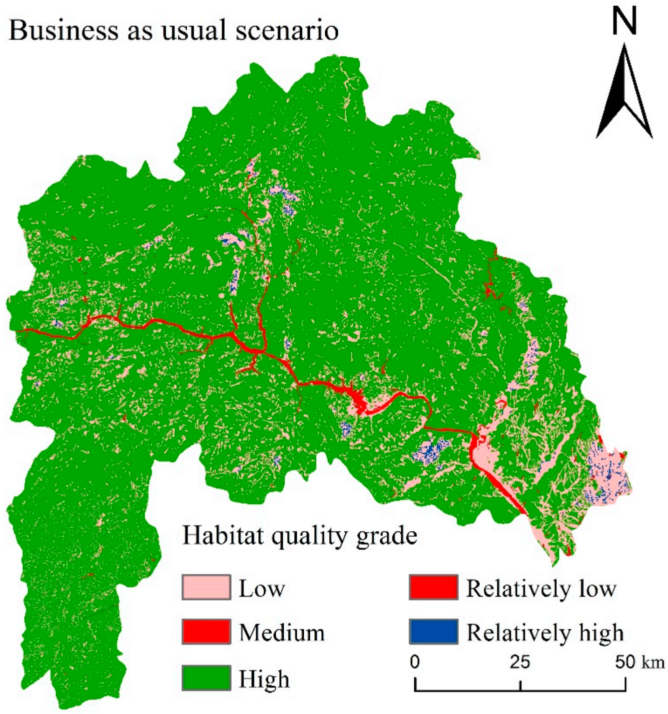

Figure 12. Forecast map of habitat quality in 2020 under the business as usual scenario

Table 8. Area and percentage of habitat quality at different grades in 2020 under business as usual scenario (km^2, %)

Habitat Quality Grade	2010		2020		2010 to 2020	
	Area	Percentage	Area	Percentage	Area	Percentage
Low	1701.48	13.90	1721.38	14.06	19.90	0.16
Relatively low	153.90	1.26	152.28	1.24	−1.62	−0.02
Medium	36.27	0.30	33.57	0.28	−2.70	−0.02
Relatively high	65.39	0.53	59.99	0.49	−5.40	−0.04
High	10,287.91	84.02	10,274.39	83.92	−13.52	−0.10

Figure 13 exhibits the future map of habitat quality under the ecological protection scenario. The variation of habitat quality in this scenario represented reverse trend to the previous decades. The overall score of habitat quality increased slightly with an increasing area of high and relatively high habitat quality grade in some local regions (Table 9). Habitat quality achieved a score of 0.8155 in 2020, and increased by 0.001 when compared with 2010. The area of landscape with high and relatively high habitat quality grade continuously increased and the area of landscape with low habitat quality grade continuously decreased. By 2020, the areas with relatively high and relatively high grade of habitat quality occupied for 84.75% of the total area, with an increasing rate of 0.2% when compared with 2010. From 2010 to 2020, the transition of landscape pattern from low to high habitat quality grade occurred in some parts of the study area, with the corresponding transitions from bare land to woodland, grassland and waters. The transition of landscape pattern from low to relatively high habitat quality grade occurred with the corresponding transitions from farmland and shoaly land to woodland and grassland. The changes were mainly concentrated in the northwestern areas of Zigui county, the northern areas of Badong county, and the shoaly areas along the Yangtze River in main urban areas of Yichang city. From 2010 to 2020, the policy implementation of returning farmland to forest may lead to the transition of paddy field and dry land to woodland. The enhancement of ecological protection awareness and series policies on vegetation protection would bring about the transition of shoaly land and bare land to woodland. The policy implementation of returning farmland to forest and the enhancement of ecological protection awareness would contribute the continuously increase of habitat quality as a whole.

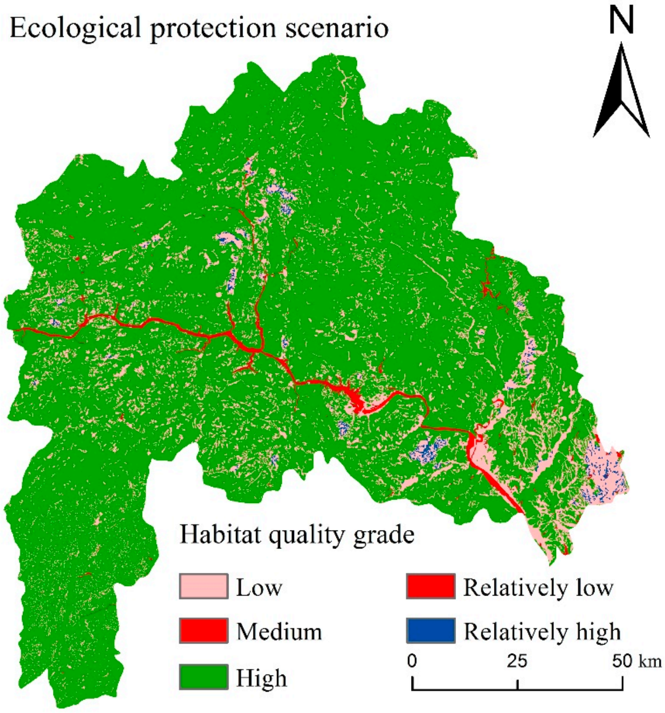

Figure 13. Forecast map of habitat quality in 2020 under the ecological protection scenario

Table 9. Area and percentage of habitat quality at different grades in 2020 under ecological protection scenario (km^2, %)

Habitat Quality Grade	2010		2020		2010 to 2020	
	Area	Percentage	Area	Percentage	Area	Percentage
Low	1701.48	13.90	1681.52	13.73	−19.96	−0.17
Relatively low	153.90	1.26	148.34	1.21	−5.57	−0.05
Medium	36.27	0.30	31.59	0.26	−4.68	−0.04
Relatively high	65.39	0.53	72.78	0.61	7.39	0.08
High	10,287.91	84.02	10,301.95	84.14	14.04	0.12

4. Discussion

This study provides an effective way to monitor the evolution of landscape pattern and habitat quality, and understand the influence of landscape pattern dynamics on biodiversity in Hubei section of TGRA. However, it should be noted that the results must be interpreted with caution.

The world-famous Three Gorges Project (TGP) is the largest hydropower station in the world and also the largest water resources and hydropower project constructed in China. The construction of TGP will generate enormous benefits in flood control, power generation, shipping and water supply, however, also may have a long-term and far-reaching impact on the ecology and environment of TGRA. The construction of the 180-m-tall dam was officially started in 1994 and the water level rise to 175 m after the three Gorges Reservoir impoundment in 2009. The study period from 1990 to 2010 we selected can fully cover the time span of Three Gorges Dam project. From 1900 to 2010, the variation of the landscape and the value of habitat degradation index seem minimal, while the value of habitat quality exhibits relatively high scores. Given that a small variation of landscape pattern occurred, however, the area of construction land has increased more than 79.46%, showing the increasing effect of human activity. The rising value of habitat degradation index and decreasing value of habitat quality can explain the degrading trend of habitat quality in study area.

Generally, the impacts of Three Gorges Dam project on biodiversity and habitat quality are far-reaching and lasting, which cannot be ignored. Compared to other similar study results [69–71], dam construction has serious consequences for aquatic ecosystems, especially in fish species and habitat area, leading to an inevitable extirpation of small, dammed-off populations, degrading habitat and fragmentation of landscape. As for biodiversity, many scholars showed evidences of pervasive biodiversity decline in this region [12–14]. The declined value of habitat quality index over the past 20-year could exhibited the impacts of Three Gorges Dam project on habitat quality, which agreed with these above conclusions. Biodiversity measurement over large areas in traditional way by calculating the number of a species in a given area [72] is far more costly and time consuming. Thus, this study could provide possibility for measuring regional alterations in biodiversity by analyzing the variation of habitat quality through remote sensing technology.

When monitoring landscape pattern dynamics, precise spatial and temporal information is required. Landsat data has been used for land-use or landscape pattern mapping in many previous studies [22,45,73,74]. The remote sensing data source in this study are mainly from Landsat-5 TM in summer time. However, a spatial resolution of 30 m and inconsistent acquisition time would affect the accuracy of the extraction results for landscape pattern. The acquisition time of remote sensing images would influence the extraction accuracy of waters. The water level of reservoirs and canals variated seasonally in a year. The extraction areas of waters from remote sensing data in flood period is generally bigger than in dry period. The results could change depending on the spatial-temporal resolution and the acquisition time of remote sensing images.

Given the lack of consideration of policy intervention impact on the landscape pattern, the future pattern prediction simulated by CA-Markov model obtained non-ideal performances under the ecological protection scenario. It is hard to quantify the effect of the policies [75–77], such as returning farmland to forestry, eco-migration policies [78], and check the coverage of all kinds of nature protection zones in space. Thus, the influence of policy intervention on landscape variation were not considered as a restriction factor. Similar studies of the influence of policy intervention on landscape variation were also found using a CA Markov model [79,80], which showed a positive impact of the National forest policy on the forest cover. If the quantified policy intervention added into the simulation model and succeed in reality, then post 2020 we expect more accurate landscape prediction and regional natural environment optimization.

As a proxy for biodiversity, habitat quality in InVEST model refers to the ability of the environment to provide conditions appropriate for individual and population persistence [81–83]. The model assumes that areas with high habitat quality grade have higher biodiversity. Once similar habitats are destroyed, biodiversity is lost [5]. However, areas with good habitat quality do not necessarily have high biodiversity. Moreover, the principle of this module is more inclined to vegetation diversity, which has certain limitations in the study area. In addition, we should recognize that a landscape has an artificial boundary where the habitat threats immediately outside of the study boundary have been clipped and ignored. Consequently, the threat intensity on the edges of a given landscape will always be less. All threats in InVEST model are additive, in some cases, the collective impact of multiple threats may be much greater than the sum of individual threat levels would suggest, which collective impact is not considered in InVEST model.

5. Conclusions

The objective of this research was to investigate the evolution of landscape pattern and habitat quality, and explore biodiversity responses under the influence of landscape pattern dynamics in Hubei section of TGRA. Several conclusions were made as follow. The overall landscape pattern has a slight but obvious change from 1990 to 2010. Terrain and climate were the most influencing natural factors compared with human factors. CA-Markov model performed well in future landscape prediction by setting socio-economic factors as restriction factor. The quality habitat has been declining over the past 20 years. Simulated habitat quality maps exhibited two opposite trends to the previous decade, indicating the impact of landscape pattern dynamics on biodiversity. The findings from this article offer the potential to analyze the impact of landscape pattern dynamics on habitat quality, and provide scientific basis for optimizing regional natural environment, as well as effective decision-making support to local government for landscape planning and management, regional biodiversity conservation, and economic sustainable development.

Author Contributions: Conceptualization, L.C., T.W. and Z.L.; methodology, L.C.; software L.C. and T.S.; validation, L.C. and T.S.; formal analysis T.S.; investigation, L.C. and Z.L.; Resources, C.C.; Writing-original draft, L.C.; Writing-review & editing, L.C. and T.W.; Supervision, C.C.; project administration, Z.L. and L.C.; funding acquisition, Z.L. and L.C.

Funding: This research was funded by the National Key Research and Development Program of China [grant numbers 2017YFC0505302], the National Natural Science Foundation of China [grant numbers 41877071], the Fundamental Research Funds for the Central Universities Project of China [grant numbers 2662016QD030].

Conflicts of Interest: The authors declare no conflict of interest.

References

1. Daily, G.C.; Polasky, S.; Goldstein, J.; Kareiva, P.M.; Mooney, H.A. Ecosystem services in decision making: Time to deliver. *Ecol. Environ.* **2009**, *7*, 21–28. [CrossRef]
2. Brath, A.; Montanari, A.; Moretti, G. Assessing the effect on flood frequency of land use change via hydrological simulation (with uncertainty). *J. Hydrol.* **2006**, *324*, 141–153. [CrossRef]
3. Bormann, H.; Breuer, L.; Gräff, T.; Huisman, J.A. Analysing the effects of soil properties changes associated with land use changes on the simulated water balance: A comparison of three hydrological catchment models for scenario analysis. *Ecol. Model.* **2007**, *209*, 29–40. [CrossRef]
4. Potschin, M.B.; Hainesyoung, R.H. Ecosystem services. *Prog. Phys. Geogr.* **2011**, *35*, 575–594. [CrossRef]
5. Tallis, H.; Ricketts, T.; Nelson, E.; Ennaanay, D. *InVEST 1.005 Beta Users Guide*; The Natural Capital Project; Stanford University: Stanford, CA, USA, 2009.
6. Hunsaker, C.T.; O'Neill, R.V.; Jackson, B.L.; Timmins, S.P.; Levine, D.A. Sampling to characterize landscape pattern. *Landsc. Ecol.* **1994**, *9*, 207–226. [CrossRef]
7. Vitousek, P.M.; Mooney, H.A.; Lubchenco, J. Human domination of Earth's ecosystems. *Science* **1997**, *277*, 494–499. [CrossRef]
8. Wilcove, D.S.; Rothsetin, D.; Dubow, J.; Phillips, A.; Losos, E. Quantifying Threats to Imperiled Species in the United States Assessing the relative importance of habitat destruction, alien species, pollution, overeplotiation, and disease. *Bioscience* **1998**, *48*, 607–615. [CrossRef]
9. Nüsser, M. Change and persistence: Contemporary landscape transformation in the Nanga Parbat region, northern Pakistan. *Mt. Res. Dev.* **2000**, *20*, 348–355. [CrossRef]
10. Fairbanks, D.H.K.; Benn, G.A. Identifying regional landscapes for conservation planning: A case study from KwaZulu-Natal, South Africa. *Landsc. Urban Plan.* **2000**, *50*, 237–257. [CrossRef]
11. Sitzia, T.; Semenzato, P.; Trentanovi, G. Natural reforestation is changing spatial patterns of rural mountain and hill landscapes: A global overview. *For. Ecol. Manag.* **2010**, *259*, 1354–1362. [CrossRef]
12. López-Pujol, J.; Ren, M.X. Biodiversity and the Three Gorges Reservoir: A troubled marriage. *J. Nat. Hist.* **2009**, *43*, 2765–2786. [CrossRef]
13. Wu, J.; Huang, J.; Han, X.; Xie, Z.; Gao, X.; Fangliang, H. Three-Gorges Dam–experiment in habitat fragmentation? *Science* **2003**, *300*, 1239–1240. [CrossRef] [PubMed]
14. Wu, J.; Huang, J.; Han, X.; Gao, X.; He, F.; Jiang, M.; Jiang, Z.; Primack, R.B.; Shen, Z. The Three Gorges Dam: an ecological perspective. *Ecol. Environ.* **2004**, *2*, 241–248. [CrossRef]
15. Kittinger, J.N.; Coontz, K.M.; Yuan, Z.; Han, D.; Zhao, X.; Wilcox, B.A. Toward holistic evaluation and assessment: Linking ecosystems and human well-being for the three gorges dam. *EcoHealth* **2009**, *6*, 601–613. [CrossRef] [PubMed]
16. Scheller, R.M.; Domingo, J.B.; Sturtevant, B.R.; Williams, J.S.; Rudy, A. Design, development, and application of LANDIS-II, a spatial landscape simulation model with flexible temporal and spatial resolution. *Ecol. Model.* **2007**, *201*, 409–419. [CrossRef]

17. Wang, X.; Yu, S.; Huang, G.H. Land allocation based on integrated GIS-optimization modeling at a watershed level. *Landsc. Urban Plan.* **2004**, *66*, 61–74. [CrossRef]
18. Baldwin, D.J.B.; Weaver, K.; Schnekenburger, F.; Perera, H.A. Sensitivity of landscape pattern indices to input data characteristics on real landscapes: Implications for their use in natural disturbance emulation. *Landsc. Ecol.* **2004**, *19*, 255–271. [CrossRef]
19. Agarwal, D.K.; Silander, J.A., Jr.; Gelfand, A.E.; Dewar, R.E. Tropical deforestation in Madagascar: Analysis using hierarchical, spatially explicit, Bayesian regression models. *Ecol. Model.* **2005**, *185*, 105–131. [CrossRef]
20. Syphard, A.D.; Clarke, K.C.; Franklin, J. Using a cellular automaton model to forecast the effects of urban growth on habitat pattern in southern California. *Ecol. Complex.* **2005**, *2*, 185–203. [CrossRef]
21. Bolliger, J.; Wagner, H.; Turner, M.G. *Identifying and Quantifying Landscape Patterns in Space and Time*; A Changing World; Springer: Dordrecht, The Netherlands, 2007; pp. 177–194.
22. Fan, F.; Wang, Y.; Wang, Z. Temporal and spatial change detecting (1998–2003) and predicting of land use and land cover in Core corridor of Pearl River Delta (China) by using TM and ETM+ images. *Environ. Monit. Assess.* **2008**, *137*, 127–147. [CrossRef] [PubMed]
23. Sang, L.; Zhang, C.; Yang, J.; Zhu, D.; Yun, W. Simulation of land use spatial pattern of towns and villages based on CA-Markov model. *Math. Comput. Model.* **2011**, *54*, 938–943. [CrossRef]
24. Batty, M.; Xie, Y.; Sun, Z. Modeling urban dynamics through GIS-based cellular automata. *Comput. Environ. Urban Syst.* **1999**, *23*, 205–233. [CrossRef]
25. Nourqolipour, R.; Shariff, A.R.B.M.; Balasundram, S.K.; Ahmad, N.B.; Sood, A.M. A GIS-based model to analyze the spatial and temporal development of oil palm land use in Kuala Langat district, Malaysia. *Environ. Earth Sci.* **2015**, *73*, 1687–1700. [CrossRef]
26. Boumans, R.; Costanza, R. The multiscale integrated Earth Systems model (MIMES): The dynamics, modeling and valuation of ecosystem services. *Glob. Water Syst. Res.* **2008**, *2*, 1.
27. Mohan, C.; Levine, F. ARIES/IM: An efficient and high concurrency index management method using write-ahead logging. *ACM Sigmod Record* **1992**, *21*, 371–380. [CrossRef]
28. Wang, Y.; Bakker, F.; Groot, R.D.; Wörtche, H. Effect of ecosystem services provided by urban green infrastructure on indoor environment: A literature review. *Build. Environ.* **2014**, *77*, 88–100. [CrossRef]
29. Natural Capital Project. Available online: https://naturalcapitalproject.stanford.edu (accessed on 14 May 2017).
30. Haunreiter, E.; Cameron, D. Mapping Ecosystem Services in the Sierra Nevada, CA. *Nat. Conserv. Calif. Program* **2011**, *12*, 16–32.
31. Mdk, L.; Matlock, M.D.; Cummings, E.C.; Nalley, L.L. Quantifying and mapping multiple ecosystem services change in West Africa. *Agric. Ecosyst. Environ.* **2013**, *165*, 6–18.
32. Terrado, M.; Sabater, S.; Chaplin-Kramer, B.; Mandle, L.; Ziv, G. Model development for the assessment of terrestrial and aquatic habitat quality in conservation planning. *Sci. Total. Environ.* **2016**, *540*, 63–70. [CrossRef] [PubMed]
33. Chen, K.Y. Ecosystem health: ecological sustainability target of strategic environment assessment. *J. For. Res.* **2003**, *14*, 146–150.
34. Zhang, M.; Jin, H.; Cai, D.; Jiang, C. The comparative study on the ecological sensitivity analysis in Huixian karst wetland, China. *Procedia Environ. Sci.* **2010**, *2*, 386–398.
35. United States Geological Survey (USGS). Available online: https://glovis.usgs.gov (accessed on 11 July 2017).
36. United States Geological Survey (USGS). Global Data Explorer. Available online: https://gdex.cr.usgs.gov/gdex/ (accessed on 21 October 2017).
37. Meteorological Data Sharing Service System of China. Available online: http://data.cma.cn/ (accessed on 30 December 2017).
38. Elvidge, C.D. Mapping City Lights with Nighttime Data from the DMSP Operational Linescan System. *Photogramm. Eng. Remote Sens.* **1997**, *63*, 727–734.
39. Zhao, G.; Dai, Z.; Hu, Y. The Suitability of Different Nighttime Light Data for GDP Estimation at Different Spatial Scales and Regional Levels. *Sustainability* **2017**, *9*, 305.
40. National Oceanic and Atmospheric Administration (NOAA). Available online: https://www.ngdc.noaa.gov/eog/dmsp/downloadV4composites.html (accessed on 9 January 2018).
41. Hulst, R.V. On the dynamics of vegetation: Markov chains as models of succession. *Vegetation* **1979**, *40*, 3–14. [CrossRef]

42. Yang, X.; Zheng, X.Q.; Lv, L.N. A spatiotemporal model of land use change based on ant colony optimization, Markov chain and cellular automata. *Ecol. Model.* **2012**, *233*, 11–19. [CrossRef]
43. Hou, W.; Walz, U. Enhanced analysis of landscape structure: Inclusion of transition zones and small-scale landscape elements. *Ecol. Indic.* **2013**, *31*, 15–24. [CrossRef]
44. Ichikawa, K.; Okubo, N.; Okubo, S.; Takeuchi, K. Transition of the satoyama, landscape in the urban fringe of the Tokyo metropolitan area from 1880 to 2001. *Landsc. Urban Plan.* **2006**, *78*, 398–410. [CrossRef]
45. Luo, G.; Amuti, T.; Zhu, L.; Mambetov, B.T.; Maisupova, B. Dynamics of landscape patterns in an inland river delta of Central Asia based on a cellular automata-Markov model. *Reg. Environ. Chang.* **2015**, *15*, 277–289. [CrossRef]
46. Hu, X.L.; Xu, L.; Zhang, S.S. Land use pattern of Dalian City, Liaoning Province of Northeast China based on CA-Markov model and multi-objective optimization. *Chin. J. Appl. Ecol.* **2013**, *24*, 1652.
47. Bayliss, J.L.; Simonite, V.; Thompson, S. The use of probabilistic habitat suitability models for biodiversity action planning. *Agric. Ecosyst. Environ.* **2005**, *108*, 228–250. [CrossRef]
48. Holzkämper, A.; Lausch, A.; Seppelt, R. Optimizing landscape configuration to enhance habitat suitability for species with contrasting habitat requirements. *Ecol. Model.* **2006**, *198*, 277–292. [CrossRef]
49. Seabrook, L.; Mcalpine, C.; Rhodes, J.; Baxter, G.; Bradley, A. Determining range edges: Habitat quality, climate or climate extremes? *Divers. Distrib.* **2014**, *20*, 95–106. [CrossRef]
50. Almpanidou, V.; Mazaris, A.D.; Mertzanis, Y.; Avraam, I.; Antoniou, I. Providing insights on habitat connectivity for male brown bears: A combination of habitat suitability and landscape graph-based models. *Ecol. Model.* **2014**, *286*, 37–44. [CrossRef]
51. Mckinney, M.L. Influence of settlement time, human population, park shape and age, visitation and roads on the number of alien plant species in protected areas in the USA. *Divers. Distrib.* **2002**, *8*, 311–318. [CrossRef]
52. Forman, R.T.T.; Sperling, D.; Bissonette, J.A. Road Ecology: Science & Solutions. *Landsc. Ecol.* **2004**, *19*, 563–565.
53. Forman, R.T.T. Some general principles of landscape and regional ecology. *Landsc. Ecol.* **1995**, *10*, 133–142. [CrossRef]
54. Lindenmayer, D.; Cunningham, R.; Macgregor, C.; Crane, M.; Michael, D. Temporal Changes in Vertebrates during Landscape Transformation: A Large-Scale "Natural Experiment". *Ecol. Monogr.* **2008**, *78*, 567–590. [CrossRef]
55. Atkinson, P.M.; Massari, R. Generalized linear modeling of susceptibility to landsliding in the central Apennines, Italy. *Comput. Geosci.* **1998**, *24*, 373–385. [CrossRef]
56. Pontius, R. Quantification Error versus Location Error in Comparison of Categorical Maps. *Photogramm. Eng. Remote. Sens.* **2000**, *66*, 1011–1016.
57. Menard, S.W. *Applied Logistic Regression Analysis (Quantitative Applications in the Social Sciences)*; SAGE Publications: Thousand Oaks, CA, USA, 2013.
58. Lee, S. Application of logistic regression model and its validation for landslide susceptibility mapping using GIS and remote sensing data. *Int. J. Remote Sens.* **2005**, *26*, 1477–1491. [CrossRef]
59. Ohlmacher, G.C.; Davis, J.C. Using multiple logistic regression and GIS technology to predict landslide hazard in northeast Kansas, USA. *Eng. Geol.* **2003**, *69*, 331–343. [CrossRef]
60. Shu, B.; Zhang, H.; Li, Y.; Qu, Y.; Chen, L. Spatiotemporal variation analysis of driving forces of urban land spatial expansion using logistic regression: A case study of port towns in Taicang City, China. *Habitat Int.* **2014**, *43*, 181–190. [CrossRef]
61. Hu, Z.; Lo, C.P. Modelling urban growth in Atlanta using logistic regression. *Comput. Environ. Urban Syst.* **2007**, *31*, 667–688. [CrossRef]
62. Ozdemir, A. Using a binary logistic regression method and GIS for evaluating and mapping the groundwater spring potential in the Sultan Mountains (Aksehir, Turkey). *J. Hydrol.* **2011**, *405*, 123–136. [CrossRef]
63. Ayalew, L.; Yamagishi, H. The application of GIS-based logistic regression for landslide susceptibility mapping in the Kakuda-Yahiko Mountains, Central Japan. *Geomorphology* **2005**, *65*, 15–31. [CrossRef]
64. Dai, F.; Lee, C.F. Landslides on Natural Terrain: Physical Characteristics and Susceptibility Mapping in Hong Kong. *Mt. Res. Dev.* **2002**, *22*, 40–47. [CrossRef]
65. Rgjr, P.; Schneider, L.C. Land-cover change model validation by a ROC method for the Ipswich watershed, Massachusetts, USA. *Agric. Ecosyst. Environ.* **2001**, *85*, 239–248.

66. Guzzetti, F.; Cardinali, M.; Carrara, A.; Reichenbach, P. Use of GIS Technology in the Prediction and Monitoring of Landslide Hazard. *Nat. Hazards* **1999**, *20*, 117–135.
67. Lee, S.; Min, K. Statistical analysis of landslide susceptibility at Yongin, Korea. *Environ. Geol.* **2001**, *40*, 1095–1113. [CrossRef]
68. Dabbaghian, V.; Jackson, P.; Spicer, V.; Wuschke, K. A cellular automata model on residential migration in response to neighborhood social dynamics. *Math. Comput. Model.* **2010**, *52*, 1752–1762. [CrossRef]
69. Morita, K.; Yamamoto, S. Effects of Habitat Fragmentation by Damming on the Persistence of Stream-Dwelling Charr Populations. *Conserv. Boil.* **2010**, *16*, 1318–1323. [CrossRef]
70. Hall, C.J.; Jordaan, A.; Frisk, M.G. The historic influence of dams on diadromous fish habitat with a focus on river herring and hydrologic longitudinal connectivity. *Landsc. Ecol.* **2011**, *26*, 95–107. [CrossRef]
71. Santuccijr, V.; Gephard, S.; Pescitelli, S. Effects of Multiple Low-Head Dams on Fish, Macroinvertebrates, Habitat, and Water Quality in the Fox River, Illinois. *N. Am. J. Fish. Manag.* **2005**, *25*, 975–992. [CrossRef]
72. Harper, J.L.; Hawksworth, D.L. Biodiversity: Measurement and estimation. *Philos. Trans. R. Soc. Lond.* **1994**, *345*, 5. [CrossRef] [PubMed]
73. Rey-Benayas, J.M.; Pope, K.O. Landscape Ecology and Diversity Patterns in the Seasonal Tropics from Landsat TM Imagery. *Ecol. Appl.* **1995**, *5*, 386–394. [CrossRef]
74. Jabbar, M.T.; Shi, Z.H.; Wang, T.W.; Cai, C.F. Vegetation Change Prediction with Geo-Information Techniques in the Three Gorges Area of China. *Pedosphere* **2006**, *16*, 457–467. [CrossRef]
75. Mcneely, J.A. *Expanding Partnerships in Conservation*; Island Press: Washington, DC, USA, 1995.
76. Chape, S.; Harrison, J.M.; Lysenko, I. Measuring the extent and effectiveness of protected areas as an indicator for meeting global biodiversity targets. *Philos. Trans. Boil. Sci.* **2005**, *360*, 443–455. [CrossRef] [PubMed]
77. Hockings, M.; Stolton, S.; Leverington, F.; Dudley, N.; Courrau, J. Assessing Effectiveness—A Framework for Assessing Management Effectiveness of Protected Areas. *Arch. Pediatr. Urug.* **2007**, *71*, 5–9.
78. Lu, Q.; Ning, J.; Liang, F.; Bi, X. Evaluating the Effects of Government Policy and Drought from 1984 to 2009 on Rangeland in the Three Rivers Source Region of the Qinghai-Tibet Plateau. *Sustainability* **2017**, *9*, 1033. [CrossRef]
79. Nagendra, H. Drivers of regrowth in South Asia's human impacted forests. *Curr. Sci.* **2009**, *97*, 1586–1592.
80. Adhikari, S.; Southworth, J. Simulating Forest Cover Changes of Bannerghatta National Park Based on a CA-Markov Model: A Remote Sensing Approach. *Remote Sens.* **2012**, *4*, 3215–3243. [CrossRef]
81. Sharma, R.; Nehren, U.M.; Rahman, S.A.; Meyer, M.; Baral, H. Modeling Land Use and Land Cover Changes and Their Effects on Biodiversity in Central Kalimantan, Indonesia. *Land* **2018**, *7*, 57. [CrossRef]
82. Nelson, E.; Mendoza, G.; Regetz, J.; Polasky, S.; Tallis, H. Modeling multiple ecosystem services, biodiversity conservation, commodity production, and tradeoffs at landscape scales. *Front. Ecol. Environ.* **2009**, *7*, 4–11. [CrossRef]
83. Nelson, E.J.; Daily, G.C. Modelling ecosystem services in terrestrial systems. *F1000 Biol. Rep.* **2010**, *2*, 53. [CrossRef] [PubMed]